Thiol Ester Hydrolysis Catalyzed by Glutathione *S*-Transferase A1-1†

Eric C. Dietze,[‡,§] Mark P. Grillo,[§,||] Thomas Kalhorn,[⊥] Brenda S. Nieslanik,[‡] Claudia M. Jochheim,[@] and William M. Atkins*[,‡]

Departments of Medicinal Chemistry and Pharmaceutics, Box 357610, University of Washington, Seattle, Washington 98195-7610, Department of Biopharmaceutical Sciences, University of California at San Francisco, San Francisco, California 94143, and Immunex Corporation, 51 University Street, Seattle, Washington 98101

Received May 28, 1998; Revised Manuscript Received August 25, 1998

ABSTRACT: rGSTA1-1 has been shown to catalyze the hydrolysis of the thiol ester glutathionyl ethacrynate (E-SG). In contrast, neither the retro-Michael addition with the substrate EA-SG, to yield GSH and ethacrynic acid (EA), nor the conjugation reaction between GSH and EA to yield the thiol ester E-SG was catalyzed to any measurable extent under similar conditions. The steady state k_{cat} and K_M for hydrolysis of E-SG by wild type rGSTA1-1 were 0.11 ± 0.009 min^{-1} and 15.7 ± 1.6 mM, respectively. The site-directed mutant, Y9F, in which the catalytic Tyr-9 is substituted with Phe, was completely inactive in this reaction. To uncover a mechanistic signature that would distinguish between direct hydrolysis and covalent catalysis involving acylation of Tyr-9, solvent isotope exchange and mass spectrometry experiments were performed. No ^{18}O incorporation into the starting thiol ester was detected with initial velocity solvent isotope exchange experiments. However, covalent adducts corresponding to acylated protein also were not observed by electrospray ionization mass spectrometry, even with an assay that minimized the experimental dead time and which allowed for detection of *N*-acetyltyrosine acylated with EA in a chemical model system. The k_{on} and k_{off} rate constants for association and dissociation of E-SG were determined, by stopped flow fluorescence, to be 5×10^5 s^{-1} M^{-1} and 6.7 s^{-1}, respectively. Together with the isotope partitioning results, these rate constants were used to construct partial free energy profiles for the GST-catalyzed hydrolysis of E-SG, assuming that Tyr-9 acts as a general acid−base catalyst. The "one-way flux" of the thiol esterase reaction results directly from the thermodynamic stability of the products after rate-limiting attack of the thiol ester by H_2O or Tyr-9, and is sufficient to drive the hydrolysis to completion, in contrast to GST-catalyzed breakdown of other GSH conjugates.

The glutathione *S*-transferases (GSTs)[1] catalyze the nucleophilic conjugation of the tripeptide glutathione (GSH) with xenobiotics and endogenous electrophiles, including drugs, toxins, and prostaglandins (*1*−*3*). As a result of their central role in detoxication, and a putative role in GSH-dependent tumor cell resistance to electrophilic chemotherapeutic agents (*4*), the GSTs have been the recent focus of intense structural, mechanistic, and clinical research (*5*−*7*). Although differences in active site topology clearly result in variable substrate selectivities between individual isozymes, the catalytic mechanism appears to be highly conserved. Specifically, an active site tyrosine or serine hydrogen bonds to, and stabilizes, the nucleophilic GS$^-$ thiolate in each of the cytosolic GSTs (*8*−*10*). The resulting GS$^-$ thiolate reacts readily with an extraordinary range of electrophilic functional groups.

In addition to conjugation reactions, however, GSTs also catalyze the release of GSH from its conjugates, as required by the Haldane relationship. Examples of "reverse" GST reactions have been limited to retro-Michael additions (*11*), and hydrolysis of activated carbamate thiol esters and thiocarbamate thiol esters formed from GSH conjugation with isocyanates and isothiocyanates, respectively (*12*−*14*). The reverse reactions are of therapeutic and toxicological importance, because the generation of GSH and an electrophile from GSH conjugates represents a potential pathway for delivery of "latent" toxins or drugs to tissues remote from the initial conjugation reaction, whether release of the conjugate is mediated by GSTs or by nonenzymatic processes (*14*, *15*). By analogy, reverse GST reactions may be exploited for novel therapeutic strategies. Traditional strategies for designing GST inhibitors have relied on formation of GSH conjugates that form reversible complexes with GSTs. However, GST-catalyzed release of reactive agents from GSH conjugates could provide a mechanism for tumor-specific drug delivery of GST inhibitors or cytotoxic agents. For these reasons, it is essential to understand the extent to which GSTs efficiently catalyze the reverse reactions of the

† This work was supported by NIH Grants GM51210 (W.M.A. and E.C.D.), GM36653 (M.P.G.), and GM7750 (B.S.N.), NCI Grant CA18029 (T.K.), and Merck Research Labs, Rahway, NJ.

* Corresponding author. Phone: (206) 685-0379. Fax: (206) 685-3252. E-mail: winky@u.washington.edu.

‡ Department of Medicinal Chemistry, University of Washington.

§ These authors contributed equally to this work.

|| University of California at San Francisco.

⊥ Department of Pharmaceutics, University of Washington.

@ Immunex Corporation.

[1] Abbreviations: amu, atomic mass units; CDNB, 1-chloro-2,4-dinitrobenzene; EA, ethacrynic acid; E-SG, thiol ester of ethacrynic acid and glutathione; EA-SG, Michael adduct of EA and glutathione; GSH, glutathione; GST, glutathione *S*-transferase; LC, liquid chromatography; ESI-MS, electrospray ionization mass spectrometry; rGSTA1-1, GSTA1-1 isoform from rat; hGSTA1-1, GSTA1-1 isoform from human; Tyr, tyrosine; NAT, *N*-acetyltyrosine.

10.1021/bi981284r CCC: $15.00
Published on Web 10/01/1998

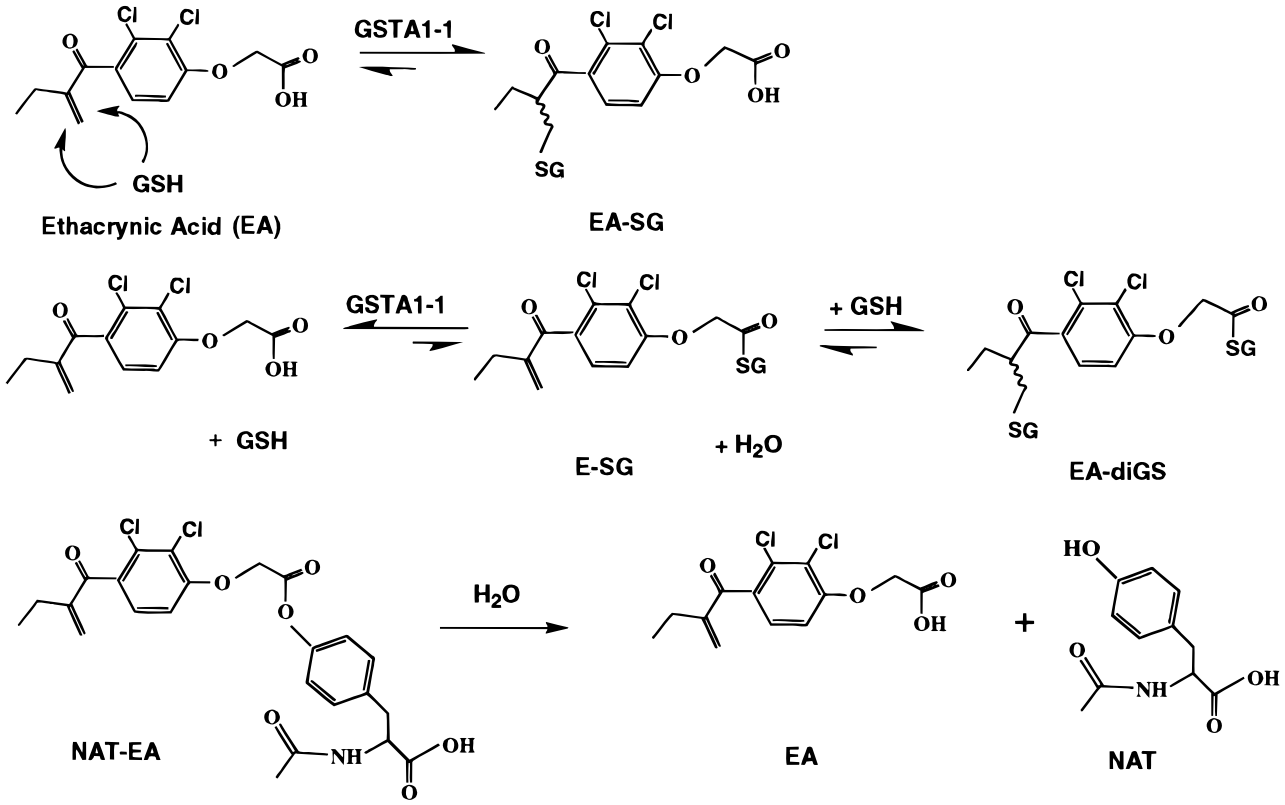

FIGURE 1: Summary of reactions studied. Michael addition of GSH to ethacrynic acid (EA) is catalyzed by several GSTs, including rGSTA1-1. The reverse reaction is not catalyzed by rGSTA1-1 under any conditions studied here, which did not include any trapping agent. The thiol ester E-SG is catalytically hydrolyzed by rGSTA1-1, although formation of the GSH thiol ester conjugate is not catalyzed by rGSTA1-1. At longer reaction times, the EA and GSH products formed by the thiol esterase activity react enzymatically and nonenzymatically to yield the EA-SG and the diadduct, EA-diGS. The reaction shown at the bottom is the hydrolysis of the ester (NAT-EA) formed from *N*-acetyltyrosine (NAT) and E-SG. NAT-EA is used here as a chemical model for a potential enzymatic intermediate formed during hydrolysis of E-SG. The nonenzymatic hydrolysis of NAT-EA is discussed along with results concerning the ESI-MS experiments with GSTA1-1 during turnover.

traditional GSH conjugation with electrophilic functional groups. However, the ability of GSTs to catalyze retroconjugation reactions remains largely unexplored. Here, we document the thiol esterase activity of GSTA1-1 toward the thiol ester formed from GSH and ethacrynic acid (glutathionyl ethacrynate, E-SG, Figure 1).

The diuretic ethacrynic acid (EA) is frequently used in vitro as a GST model substrate, wherein the Michael acceptor is the only site of GSH conjugation. EA is converted by several GST isozymes to EA-SG (*16*−*18*). Both EA and EA-SG are well-documented inhibitors of several GST isoforms. As a result, EA and EA-SG have been considered as candidates for chemotherapy adjuvants with antitumor agents that are metabolized by P-class GSTs overexpressed in tumor cells (*7*, *16*, *19*). The mechanism of GST inhibition by EA is complex and isozyme-dependent. For A- and M-class GSTs, reversible inhibition by both EA and the product EA-SG is observed (*18*). For P-class GSTs, Michael addition of EA to a cysteine thiol on the protein (Cys-47 for hGSTP1-1) yields a slowly reversible, inhibited complex, although enzyme-catalyzed formation and breakdown of EA-SG compete with this process (*16*, *17*). Formation of the thiol ester E-SG has not been reported in any incubations containing GST, EA, and GSH. During the characterization of various nonenzymatically synthesized GSH conjugates, we observed a significant GST-catalyzed hydrolysis of E-SG. The reactions that are studied in this paper are summarized in Figure 1.

The potential toxicological significance of the thiol esterase reaction lies in the precedent that it provides for metabolism of other GSH thiol esters, which are commonly found. An example of a thiol ester GSH conjugate resulting from in vivo metabolism of an administered drug is the conjugate formed with clofibrate, which may result from GSH attack of the glucuronide conjugate that is initially formed (*20*). Moreover, endogenously synthesized, hepatic, oxalyl glutathione has been proposed to regulate insulin function (*21*, *22*). Other endogenous GSH thiol esters include *S*-lactoyl GSH, *S*-succinyl GSH, and *S*-formyl GSH (*23*). In addition to these examples, GSTs presumably encounter other GSH thiol esters, and if GSTs efficiently hydrolyze a wide range of GSH esters, then these reactions must contribute to the cellular distribution and steady state levels of both GSH conjugate thiol esters and their hydrolysis products. The results presented here extend the range of GSH conjugates that are candidates for GST-mediated hydrolysis to include stabile thiol esters and provide mechanistic details about these, largely unstudied, reactions. The GST-catalyzed hydrolysis of thiol esters has not been previously reported.

MATERIALS AND METHODS

Chemicals. E-SG was synthesized by dissolving 1.6 mmol of EA in 25 mL of dry THF at room temperature and adding 1.6 mmol of triethylamine while the solution was stirred. Next, 1.6 mmol of ethyl chloroformate was added and the mixture stirred for an additional 30 min. The precipitate

was removed by filtration and the filtrate added directly to 25 mL of H_2O/THF (1:1.5) containing 1.6 mmol of GSH and 1.6 mmol of $NaHCO_3$. No enzymatic reaction products were precipitated by these conditions. The resulting mixture was stirred for 1 h at room temperature under nitrogen, at which time the reaction was terminated by the addition of 8 drops of c-HCl. The THF was removed under vacuum, and the remaining aqueous phase was extracted four times with 50 mL of ethyl acetate. The product, E-SG, was precipitated at the interface of the two layers. The E-SG was recovered and washed four times with 50 mL of water to remove unreacted GSH. The resulting product was then washed four times with 50 mL of acetone to remove unreacted EA. The final precipitate was dried under a stream of nitrogen. The resulting E-SG was pure as determined by reversed phase HPLC. The CID MS/MS spectrum in the positive ion mode of E-SG was as follows: [M + H] *m*/*z* (relative intensity) [M + H − Gly] *m*/*z* 517 (30%), [M + H − pyroglutamic acid] *m*/*z* 463 (14%), [ethacrynyl-*S*-acyl-$CH_2CH{=}NH_2$] *m*/*z* 360 (42%), [M + H − GS − CO] *m*/*z* 257 (28%), [M + H − GS − $COCH_2$] *m*/*z* 243, [pyroglutamic acid + H] *m*/*z* 130 (18%), [pyroglutamic acid − CO_2H] *m*/*z* 84 (25%), [Gly + H] *m*/*z* 76 (22%). ^{1}H NMR in DMSO-d_6 gave peaks with the following chemical shifts (in parts per million): δ 1.08 (t, 3H, J = 7.2 Hz), 1.80−1.84 (m, 2H), 2.3 (m, 2H), 2.38 (q, 2H, J = 7.2 Hz), 3.0−3.5 (m, 2H), 3.43 (m, 1H), 3.7 (m, 1H), 4.64 (m, 1H), 5.15 (s, 2H), 5.55−6.10 (2 s, 2H), 7.20−7.40 (m, 2H), 8.49 (d, 1H, J = 8.49 Hz), 8.78 (t, 1H, J = 6.6 Hz). ^{13}C NMR in DMSO-d_6 gave the following chemical shifts (in parts per million): δ 12.43 ($\underline{C}H_3CH_2$), 22.88 ($CH_3\underline{C}H_2$), 26.61 (Cys Cβ), 29.45 (Glu Cβ), 31.31 (Glu Cγ), 41.12 (Gly Cα), 51.61 (Glu Cα), 52.88 (Cys Cα), 72.99 ($OCH_2\underline{C}{=}O$), 112.20 (Ar), 127.53 (Ar), 129.47 (Ar), 132.98 (Ar), 149.25 and 154.74 (C═C), 170.06 (Cys CON), 170.24 (Glu COOH), 170.80 (Glu CON), 171.75 (Gly COOH), 195.05 (CO-Ar), 195.91 (COS).

EA-SG was synthesized by mixing 250 mg of GSH in 25 mL of H_2O with 500 mg of EA in 50 mL of 1:1 H_2O/EtOH, containing 2.5 mL of saturated $NaHCO_3$. The mixture was stirred for 24 h at room temperature. Solvents were evaporated to afford a solution in ~2 mL. Aliquots were purified by HPLC (silica) with a mobile phase of 80:20 acetonitrile/H_2O. Chromatographically pure EA-SG, obtained in 80% yield, was characterized by MS and ^{1}H NMR, and the results were consistent with the expected product.

Protein Expression, Purification, and Mutagenesis. Wild type and mutant GSTs were expressed in *Escherichia coli* strain DH5α and purified as described previously (*24*). The "wild type GST" used here is a site-directed mutant W21F, which has been previously described and which exhibits kinetic properties essentially identical to those of the "true" wild type. The Y9F mutant is a double mutant containing the W21F substitution.

Assay of Thiol Esterase Activity. GST was incubated at 25 °C with E-SG and the assay terminated by withdrawing a 200 μL aliquot at a single time point and mixing with an equal volume of stop solution (4:1:0.2 acetonitrile/methanol/formic acid). The mixture was then centrifuged to pellet precipitated GST and placed on ice. No enzymatic reaction products were precipitated by these conditions. An aliquot was also withdrawn immediately upon addition of E-SG to provide a zero time point. Parallel incubations without GST were run to correct for nonenzymatic hydrolysis of E-SG. All assays were run in triplicate. Samples were shown to be stable for more than 24 h with no detectable hydrolysis, under these conditions (data not shown).

Analysis was carried out with an isocratic HPLC system. Samples were loaded in a thermostated autoinjector (4 °C) and run with a 10 cm × 4.6 mm (inside diameter) C18 column, a mobile phase of 60% acetonitrile/methanol (1:1) and 40% 20 mM acetic acid, and a flow rate of 1 mL/min. All compounds were monitored by their absorbance at 230 nm, and the detector response was linear over the entire range of concentrations used (R^2 > 0.99, data not shown). This system allowed rapid analysis and separated E-SG from EA-SG, EA-diSG, and EA. EA, E-SG, and EA-SG standards were used to aid peak identification

Assay Optimization. The E-SG assay was performed at varying pHs, times, and GST concentrations to optimize the assay and ensure that, under the conditions employed, the assay was linear. A mixed buffer of MES, Tris, and CAPSO (50 mM each) was used, and buffers at pH 5.5 and 9.5 were blended to achieve the desired pH. The activity of GST was measured from pH 6.5 to 9.0, with 0.2−8 μM GST, and from 0 to 30 min.

Kinetics of E-SG Hydrolysis and ^{18}O Incorporation. The rate of E-SG hydrolysis was measured by incubating 1.5 μM GST for 20 min at pH 7.25 with 3.1−100 μM E-SG in triplicate in two separate assays. For quantitation, we used the HPLC system described above. For ^{18}O incorporation, conditions were the same as for kinetic measurements except that 100 μM E-SG was used in 50 mM potassium phosphate buffer (pH 7.5) and 85% $H_2{}^{18}O$. Incorporation of ^{18}O was monitored by LC−ESI-MS.

LC−ESI-MS. To follow ^{18}O incorporation and allow positive identification of peaks, an LC−ESI-MS system was used. As in the isocratic system described above, a 10 cm × 4.6 mm (inside diameter) C18 column was used and a flow rate of 1 mL/min. However, to separate all peaks from each other and the buffer salts eluting in the void volume, a linear gradient was used starting at 40% acetonitrile/methanol (1:1) from 0 to 2 min, changing to 70% acetonitrile/methanol (1:1) by 15 min, holding at 70% until 17 min, and returning to 40% acetonitrile/methanol (1:1) at 18 min. The column was re-equilibrated for 7 min between runs. A postcolumn split of 20:1 was used for introduction of the sample into the ESI-MS instrument which was run in positive ion mode.

Stopped Flow Kinetics. Stopped flow fluorescence experiments were performed with a SLM-8100 spectrofluorimeter equipped with a SLM milliflow reactor. Intrinsic tryptophan fluorescence was monitored with excitation at 295 nm and emission at 335 nm, with 2 μM GST in 50 μM MES at pH 6.5 and 14 °C. The k_{on} was determined by fitting the change in fluorescence intensity to the equation $I(t) = Ae^{-(k_{obs})t}$ at E-SG concentrations between 10 and 40 μM, where $I(t)$ is the fluorescence intensity at time t after mixing. The recovered rate constants, k_{obs}, at each E-SG concentration were plotted and fit to the equation $k_{obs} = k_{on}[\text{E-SG}] + k_{off}$. The k_{off} was determined by diluting the preformed binary complex GST·E-SG in solutions containing 2 μM GST and 20 μM E-SG with buffer containing 1 mM *S*-hexyl GSH as a trapping agent.

Mass Spectrometry with GST and a Chemical Model for Tyr-9 Acylation. Incubations containing 10 μM GST and

100 μM E-SG in 50 mM NH_4HCO_3 (pH 7.3) were loaded on a 5 cm × 4.6 mm (inside diameter) Poros R2H column (Perseptive Biosystems) interfaced with an AP1350 MS system, to separate the protein from buffer and excess ligand. A fast linear gradient from 30% acetonitrile in H_2O (0.05% TFA) at 0 min to 80% acetonitrile at 8 min was used. The orifice voltage was kept low (30 V) to minimize fragmentation. At variable times after addition of E-SG, mass spectra were obtained.

A chemical model for the acylated protein adduct was obtained by incubation of varying concentrations of *N*-acetyltyrosine and E-SG in acetonitrile, at room temperature, overnight. Reaction products were analyzed by LC−ESI-MS using a mobile phase of 50% acetonitrile/50% H_2O (0.1% acetic acid), and a C8, 15 cm, reversed phase column at a flow rate of 1 mL/min. The orifice voltage was 80 V. Reaction products were the ester resulting from transacylation ($MH^+ = 508$ *m*/*z*) and GSH ($MH^+ = 307$ *m*/*z*). The ester was not obtained when EA was incubated with *N*-acetyltyrosine. The ester was purified by HPLC using the same conditions, and the purified compound was incubated at room temperature under conditions identical to those used for enzymatic reactions. At various times, aliquots were removed and analyzed by HPLC. The peak area corresponding to the ester was integrated and normalized to the "zero time" aliquot. The half-life under these conditions was determined to be 6.5 h. The ester was converted exclusively to *N*-acetyltyrosine and EA; no other products were observed.

RESULTS

Characterization of the Reaction. As part of the initial characterization of GST thiol esterase activity, the pH dependence of the reaction was determined, and compared to that of the nonenzymatic reaction. Reaction components, including GSH, E-SG, EA-SG, and EA, were chromatographically monitored as described in Materials and Methods. Whereas the nonenzymatic reaction exhibited a constant increase in rate with increasing pH, above ~pH 7.5, the enzyme-catalyzed hydrolysis of E-SG exhibited a broad pH optimum between pH 7.0 and 8.25. Therefore, further characterization of this enzymatic activity was performed at pH 7.25. Also, we observed a time- and concentration-dependent dimerization of E-SG at pHs above ~8.0, on the basis of mass spectrometric analysis. This hampered determination of V_{max} and K_M at higher pHs. Therefore, the pH profiles for the enzymatic and nonenzymatic hydrolysis reactions are summarized in Figure 2, using a single common concentration of E-SG (100 μM). Although K_M varied slightly with pH, E-SG concentrations approach saturation at each pH and the rates indicated in Figure 2 approximate closely V_{max}. Because the rates shown in Figure 2 are not true V_{max} values, the pH dependence should not be interpreted in terms of specific microscopic rate constants, and it provides only a qualitative comparison of enzymatic and nonenzymatic processes. Under the conditions used for the remainder of the experiments, the extent of formation of EA and GSH from E-SG was linear with time for at least 30 min, and dimerization of E-SG and nonenzymatic hydrolysis were negligible. Notably, we have demonstrated previously that the active site tyrosine of rGSTA1-1 is partially ionized at this pH, with a pK_a of 8.2 (*25*−*27*), and a similar pK_a has been reported for Tyr-9 of the human GSTA1-1 (*28*). The relevance of this point is discussed below.

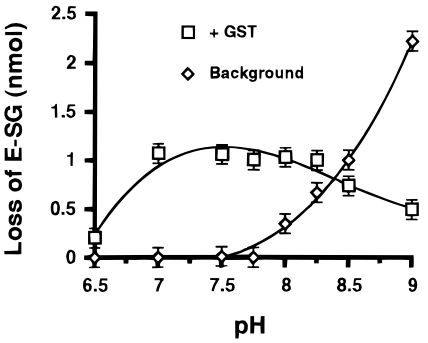

FIGURE 2: pH dependence of the GST-catalyzed and nonenzymatic hydrolysis of E-SG. The remainder of the studies described here were performed at pH 7.25. Incubations were analyzed at a single time point (20 min), and 100 μM E-SG was used in them. Less than 10% of the starting E-SG is hydrolyzed in this time. The amount of E-SG consumed does not reflect the actual V_{max} at each pH. See the text for details.

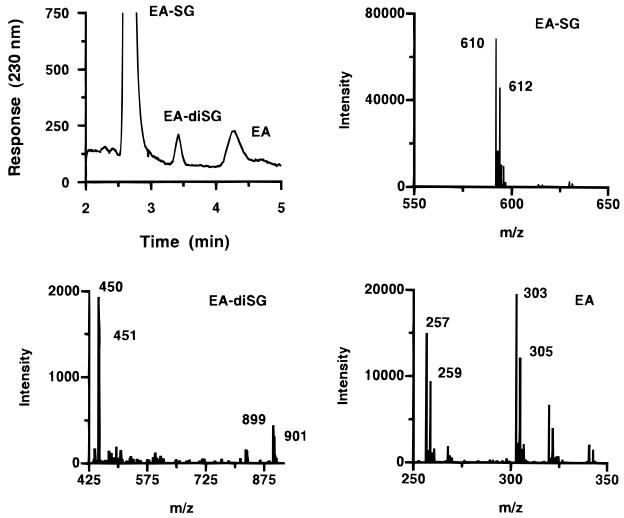

FIGURE 3: LC−MS assay for hydrolysis of E-SG. HPLC conditions are given in Materials and Methods. ESI-MS spectrum of hydrolysis products. The ESI-MS spectrum of the GST-dependent reaction product is identical to the spectrum of standard EA. In addition, the diadduct EA-diGS is formed at longer incubation times.

The identity of the reaction product EA was verified by LC−MS. The product peak coeluted with standard EA and yielded an ESI mass spectrum identical to the standard (Figure 3). The MH^+ doublet at 303 and 305 *m*/*z* reflects the expected isotopic distribution of the chlorine-containing product, as does the Na^+ adduct at 325 and 327 *m*/*z*.

The k_{cat} and K_M values for hydrolysis of EA-GS at pH 7.25 and 25 °C are summarized in Table 1. Notably, the K_M for the thiol ester is remarkably low compared to the K_Ms for GSH and many electrophilic substrates. Together with the relatively slow turnover rate, this makes E-SG a significantly more potent inhibitor in the GST-dependent metabolism of electrophiles other than EA or EA-SG. The inhibitor characteristics of E-SG will be described in detail elsewhere. Also, the EA-SG conjugate resulting from Michael addition at the terminal olefin is not converted to EA and GSH via a retro-Michael type reaction under any conditions studied, by rGSTA1-1. No EA-trapping agent was included in the incubations. Importantly, the site-directed mutant Y9F, for which the catalytic tyrosine has

Table 1: Kinetic Parameters for Reactions with Ethacrynic Acid and Analogues

system catalyst/reactant → product	K_M (μM)	k_{uncat} or k_{cat} (min^{-1})
thiol ester hydrolysis		
GST/E-SG → EA + GSH		0.0019 ± 0.0003
wild type GST/E-SG → EA + GSH	15.7 ± 1.56	0.11 ± 0.009
Y9F GST/E-SG → EA + GSH		0.0[a]
thiol ester formation		
GST/EA + GSH → E-SG		0.0
wild type GSTA1-1/EA + GSH → E-SG		0.0
GSTA1-1 Y9F/EA + GSH → E-SG		0.0
Michael addition		
GST/EA + GSH → EA-SG		0.0066 ± 0.0004
wild type GSTA1-1/EA + GSH → EA-SG	55 ± 10[b]	2.9 ± 0.1

[a] A value of 0.0 means none was detected, although it was sought. [b] The K_M reported for Michael addition is for EA at a saturating GSH concentration.

been replaced with Phe, does not catalyze detectable thiol esterase activity, thus demonstrating that this reaction occurs at the active site. The results are also summarized in Table 1.

One obvious possible mechanism of thiol esterase activity entails direct hydrolysis by active site H_2O. The complete absence of esterase activity with the Y9F mutant, together with the pK_a of Tyr-9 in the wild type, suggested the additional formal possibility that the phenolate anion of Tyr-9 could be a nucleophilic catalyst, yielding a covalently acylated protein adduct, followed by hydrolysis to regenerate the Tyr-9. To examine this possibility, enzymatic and nonenzymatic reactions were conducted in $H_2{}^{18}O$, and the ^{18}O content of the substrate E-SG was determined during turnover, by ESI-MS. The extent of solvent isotope exchange into thiol esters is highly dependent on pH, and therefore on mechanism, in nonenzymatic systems (*29*). At pHs near neutrality, little exchange is observed, due to nearly complete partitioning of the tetrahedral intermediate to products and the poor electrophilic nature of the resulting carboxylate. However, we reasoned that the active site of a GST enzyme, evolved to favor GSH conjugate formation, may demonstrate a poor commitment to catalysis in the hydrolytic direction. Upon generation of GS^- in an intimate complex with the EA carboxylate, a GST may be expected to catalyze the re-formation of the thiol ester conjugate such that the K_{int}, [GST·E-SG]/[GST·EA·GS^-], may be significantly larger than the K_{eq} for the chemical equilibrium, [E-SG]/[EA + GS^-]. Thus, initial velocity solvent isotope exchange experiments were exploited as a probe of commitment to catalysis after formation of the tetrahedral intermediate or ternary complex GST·EA·GSH. Furthermore, if GSTA1-1 catalyzed the solvent isotope exchange reaction, then this would eliminate Tyr-9 as a candidate for the initial nucleophile during the net hydrolysis. Obviously, the presence of ^{18}O in the hydrolysis product EA is required by either mechanism. The results from hydrolysis reactions conducted in $H_2{}^{18}O$ are summarized in Figure 4. Interestingly, the starting thiol ester incorporated ^{18}O in the absence of GST, albeit at a slow rate. However, under initial velocity conditions, no additional enzyme-catalyzed solvent isotope exchange was observed. In fact, the enzyme suppressed the solvent exchange reaction. This is a result of a larger fraction of the hydrolyzed products being from the GST-complexed tetrahedral intermediate when enzyme is present.

In addition, we attempted to observe catalysis of the formation of E-SG from EA and GSH. At concentrations

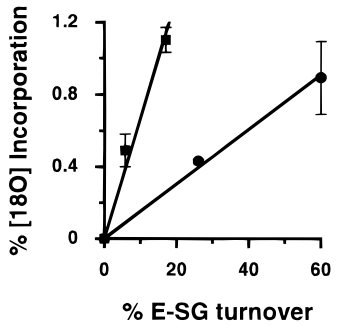

FIGURE 4: Solvent isotope partitioning vs extent of hydrolysis. The rate of ^{18}O incorporation into the starting thiol ester is plotted as a function of the extent of reaction (% E-SG hydrolyzed). In the absence of enzyme, ^{18}O incorporation into the starting thiol ester is observed (squares). In contrast, no ^{18}O incorporation above background is observed in the presence of sufficient GST to catalyze significant thiol ester hydrolysis (circles). The tetrahedral intermediate formed in the nonenzymatic reaction partitions efficiently to the starting thiol ester, or it is not derived from nucleophilic solvent. The isotopic distribution is corrected for the mole fraction of ^{18}O in the $H_2{}^{18}O$ used (0.85).

of 1 mM EA and GSH, no thiol ester was detected under a range of conditions which afforded the Michael adduct, EA-SG. Together with the results from solvent isotope experiments, the results indicate that GSTA1-1 does not catalyze to a measurable extent the conjugation of GSH to the carboxylate of EA to afford the thiol ester.

Stopped Flow Analysis of E-SG Association and Dissociation. Inasmuch as the rate of GSH conjugate dissociation is often the rate-limiting step in catalysis, particularly for A-class isoforms (*30*), and because this may control the extent of solvent isotope exchange into the thiol ester, determining the k_{off} for release of E-SG from the enzyme, and k_{on} for its association, was of interest. Therefore, the ligand-induced change in intrinsic fluorescence of Trp-21 was exploited (*31*), in stopped flow experiments (Figure 5). The determined k_{off} and k_{on} values were 6.7 s^{-1} and 5×10^5 M^{-1} s^{-1}, respectively. These results indicate that the dissociation of E-SG is sufficiently fast to expect any ^{18}O-containing thiol ester formed from the tetrahedral intermediate to dissociate from the enzyme. The E-SG is not sufficiently "sticky" to mask solvent exchange. Also, the experimentally determined rate constants, k_{on} and k_{off}, yield a kinetically determined K_D of 13.4 μM. This is nearly identical to the experimentally measured K_M, as expected for a reaction that is severely limited by the chemical step following substrate association.

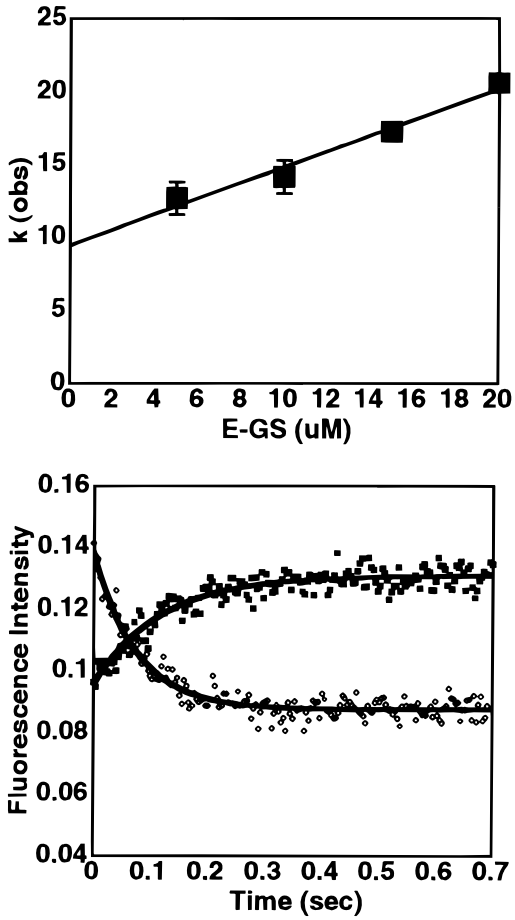

FIGURE 5: Stopped flow analysis of E-SG association and dissociation. The k_{obs} vs [E-SG] plot was used to obtain k_{on}, as described in Materials and Methods (top). Typical progress curves for the approach to equilibrium after mixing or dilution are shown (bottom): (■) dissociation and (◇) association. Solid lines are fitted curves corresponding to the determined rate constants.

Mass Spectrometry. Together, the results do not rule out the possibility that Tyr-9 acts a nucleophilic catalyst. To explicitly address this possibility, we searched for a protein adduct corresponding to acylated GST during the steady state, by using electrospray ionization mass spectrometry (ESI-MS). For these experiments, wild type GSTA1-1 and Y9F were incubated with excess E-SG under conditions identical to the assay conditions described above. At various times, aliquots were removed for analysis. A Poros reversed phase HPLC column was used to rapidly separate protein, ligand, and buffer salts with a minimum "dead" time between removal of the aliquot and ionization. The minimal dead time achieved that afforded sufficient chromatographic separation was 5.1 min, which included the chromatographic retention time of the protein. Obviously, for many enzyme-catalyzed processes, this dead time would not provide sufficient time resolution for detection of a reaction intermediate. However, the thiol ester hydrolysis described here is sufficiently slow that an acylated intermediate could be observed if the rate of deacylation corresponded to the overall turnover rate. Throughout the steady state, between 0 and 40 min after addition of E-SG to the protein, the only protein species observed by ESI-MS was the unmodified wild type or the unmodified Y9F. The recovered masses were 25391.1−25392.4 amu for the wild type and 25374.7−25375.9 amu for Y9F. The theoretical masses predicted from amino acid sequences, including the relevant amino acid substitutions, are 25391.93 and 25375.93 amu for the wild type and Y9F, respectively. No ions corresponding to the expected mass for an acylated adduct ($MH^+ + 285.14$ amu) were observed for either protein at any time during the steady state. In addition to the absence of observable acylated adducts, the chromatographic retention time of each protein was identical in the presence or absence of E-SG. Adducts such as the acylated product sought here frequently alter chromatographic retention times, but no change in retention time or peak shape was observed upon incubation with E-SG. On the basis of these observations, we concluded that a stable acylated GST adduct was not formed during the enzymatic hydrolysis of E-SG. Positive control experiments were performed in which a chemical model for the acylated Tyr was synthesized. These experiments were designed to determine whether an acylated Tyr-9, if formed, would be intrinsically unstable to such an extent that it would be hydrolyzed before ionization in the ESI-MS experiment. Specifically, E-SG was mixed with *N*-acetyltyrosine, and the chemical stabilities of the products under conditions of the assay were validated. On the basis of ESI-MS, the product obtained was the ester resulting from transacylation, with an MH^+ of 508 *m*/*z*. The transacylation product was sufficiently stable to be isolated by HPLC and was readily monitored by ESI-MS. It was found to have a half-life under these conditions of 6.5 h. Moreover, the conditions used for ESI-MS did not cause any detectable breakdown of the ester formed from *N*-acetyltyrosine and E-SG. Thus, the chemical stability of an EA-acylated Tyr-9, in the absence of enzyme-catalyzed deacylation, is sufficient to be observed by this approach. The model reaction is shown in Figure 1. It is interesting that the ester NAT-EA was not obtained directly from EA and NAT, but only from transacylation with E-SG.

Also, these experiments provided an unexpected additional "positive control". Specifically, we observed that upon incubation for ≥1 h, protein adducts were apparent. Ions corresponding to $MH^+ + 593$ amu were observed for both wild type and Y9F proteins. Presumably, these ions reflect a slow Michael addition of E-SG to the proteins at a site other than Tyr-9, which remains to be determined. These species could not be observed above baseline in the first 40 min, and their levels were found to increase with time upon incubation for longer periods of time. Because the formation of these adducts is clearly distinct temporally from the thiol ester hydrolysis, we have not pursued their identity here. However, the results do suggest that adducts formed are readily detected under the conditions used here, and they further diminish the possibility that acylated Tyr-9 is the predominant species during steady state hydrolysis by GSTA1-1. The results of the mass spectrometry experiments are summarized in Table 2. The possibility still exists that deacylation of Tyr-9 is fast relative to the dead time of the experiment, as discussed in more detail below.

DISCUSSION

rGSTA1-1 has been shown to catalyze the hydrolysis of the non-carbamate thiol ester E-SG. GSTs have been shown previously to catalyze the breakdown of GSH conjugates via retro-Michael additions, and hydrolysis of carbamate thiol esters or thiocarbamate thiol esters (*11*−*13*). Interestingly,

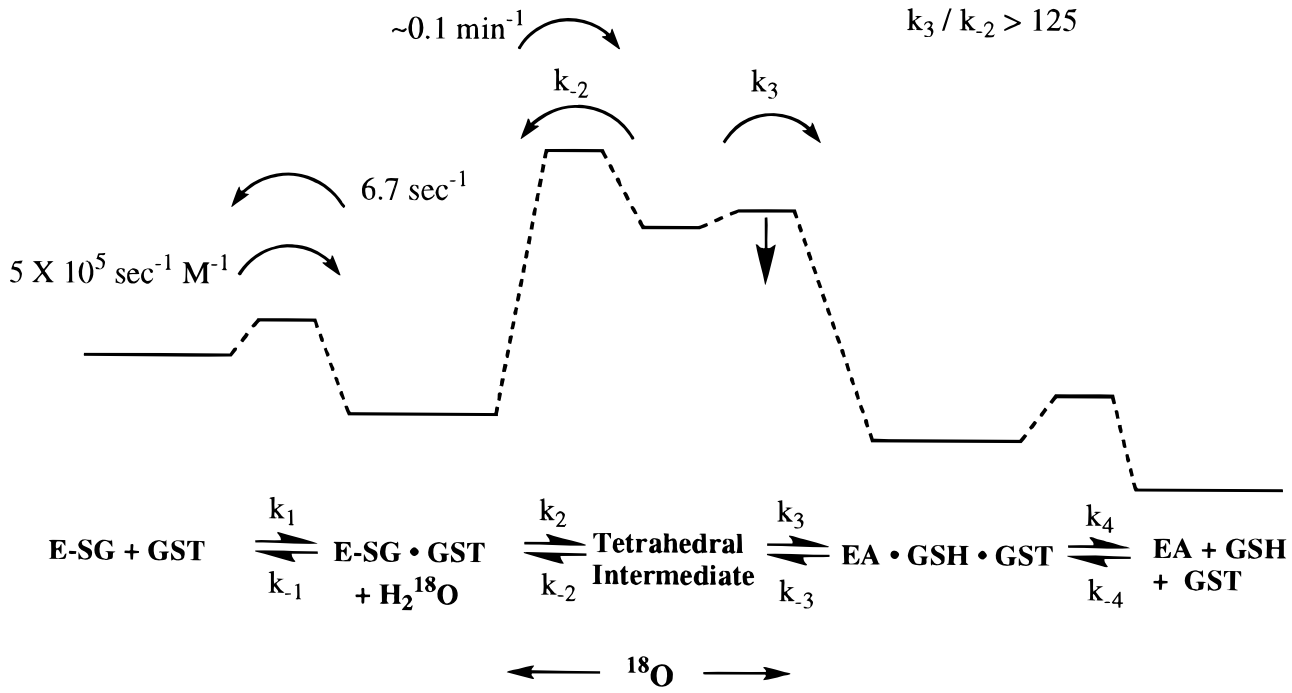

FIGURE 6: Schematic representation of a possible free energy profile for GSTA1-1-catalyzed thiol ester hydrolysis. This scheme assumes direct hydrolysis by active site H_2O, rather than nucleophilic catalysis by Tyr-9. The kinetic constants that have been experimentally determined in this work are indicated with the relevant values. The flux of the tetrahedral intermediate favors the products EA and GSH, with a k_3/k_{-2} of ≥ 125. On the basis of the data presented here, the rate-limiting step is attack of H_2O. The arrow under the kinetic barrier for k_3 is a reminder that the data provide an upper limit for this rate constant; this step may be faster. See the text for further explanation.

Table 2: Mass Spectrometry Results

protein[a]	theoretical mass of the unmodified protein (amu)	determined mass (amu)	theoretical mass of the acylated protein (amu)
wild type			
0 min[a]	25391.93	25391.1	25677.07
2−40 min		25391.1−25392.4	
60−90 min		25984.1 and 25391.6	
Y9F			
0 min	25375.93	25374.0	25661.07
2−40 min		25374.7−25375.9	
60−90 min		25967.2 and 25374.8	

[a] Times refer to the time of incubation with GSTA1-1 and E-SG, prior to chromatography on a Poros R2H reversed phase column.

GSH conjugate analogues have been exploited to deliver cytotoxic drugs to GST-expressing neoplastic cells (*32*). In these cases, however, the GST-catalyzed hydrolysis does not afford GSH as a reaction product, but rather the glutathione sulfone is obtained. In essentially all cases in which the GSH conjugate is catalytically degraded to GSH, the "forward" conjugation reaction is more efficiently catalyzed, and the GSH conjugate remains the favored product at equilibrium. In marked contrast, the GSTA1-1 isozyme does not catalyze formation of the E-SG thiol ester at a detectable rate, but the enzyme efficiently catalyzes its hydrolysis, thus driving to completion the "reverse reaction" of the traditional GST conjugation activity. This reflects the thermodynamic driving force for thiol ester hydrolysis, wherein the hydrolyzed products are favored by as much as 7−8 kcal/mol at neutral pH (*33*). This thermodynamic driving force, along with the kinetic competence of GSTs in thiol ester hydrolysis, may provide advantages for GSH-based prodrugs by ensuring that the reaction goes to completion.

Also observed in reaction mixtures containing GSTA1-1 and E-SG, at greater extents of reaction, were the EA-SG and the di-adduct, EA-diGS. The formation of EA-SG and of EA-diGS was confirmed directly by LC−MS (Figure 3). Thus, at longer incubation times and lower concentrations of E-SG, GSTA1-1 serves as an "isomerase" whereby the GSH hydrolyzed from E-SG in the thiol esterase reaction is reconjugated at the Michael acceptor to yield a net GSH transfer reaction. At the concentrations of E-SG used in these studies, this Michael addition with hydrolyzed GSH and EA does not compete significantly with E-SG for the enzyme active site, and the nonenzymatic Michael type addition predominates. Determination of the rates of these processes, and a detailed kinetic analysis of these sequential reactions, requires additional study. Here, we have focused on the thiol ester hydrolysis.

It is useful to compare the catalytic parameters for E-SG hydrolysis with those from common GST-catalyzed conjugation reactions, GST-mediated hydrolysis of GSH conjugates, and glutathione thiol esterase activity exhibited by enzymes unrelated to GSTs. For GST-catalyzed conjugation of GSH with CDNB and EA, the turnover rates observed with rGSTA1-1 are 128 (*34*) and 2.9 min^{-1}, respectively, compared to 0.11 min^{-1} for the thiol esterase reaction described here. Thus, the catalytic efficiency for thiol ester hydrolysis is relatively poor compared to that of the conjugation reaction with a "good" substrate such as CDNB, but the hydrolysis rate is comparable to those of some GST-catalyzed conjugation reactions, such as with EA. Notably, the K_M for the thiol esterase activity described here is ~25-fold lower than K_M values for common electrophilic substrates, and it is more than 1 order of magnitude smaller than the K_M for GSH in conjugation reactions (~350 μM). Interestingly, the rate of hydrolysis of E-SG by rGSTA1-1 is nearly identical to the

hGSTA1-1-catalyzed rates of hydrolysis of several GSH−isothiocyanate conjugates (*13*). Although the thiol esterase activity of rGSTA1-1 is markedly less efficient than many GST-catalyzed conjugation reactions, and nearly identical to hydrolytic rates of GSH−isothiocyanate conjugates, the "net" thiol esterase activity is significantly more efficient than the GST-mediated breakdown of GSH thiocarbamate thiol esters or retro-Michael additions, owing to the enzyme-mediated re-formation of the GSH conjugates in the latter cases (*11*−*13*).

Also, it should be noted that the thiol esterase activity reported here is significantly less efficient than that observed with other, previously characterized, GSH *S*-acyl thiol esterases, although direct comparison is difficult due to the characterization of those enzymes in crude tissue homogenates and with few recent data with cloned enzymes (*23*, *35*, *36*). Presumably, enzymes which play specific roles in the metabolism of GSH thiol esters will be more efficient than the GSTs. However, it is well appreciated that the individual GST enzymes exhibit broad substrate specificity in conjugation reactions, with pronounced differences in conjugation efficiency with different electrophiles. By analogy, it is likely that other GSH thiol esters may be catalytically hydrolyzed by GSTs with dramatic differences in kinetic parameters, and some GST thiol ester combinations may result in much faster hydrolysis.

The toxicological or therapeutic importance of thiol esterase activity described here depends on the generality of this catalysis with respect to other GSH thiol esters. The measured kinetic parameters demonstrate that, in principle, endogenous or synthetic GSH thiol esters could effectively compete with GSH for GST active sites and be hydrolyzed at a modest, but significant, rate in vivo, without GST-mediated re-formation of the starting thiol ester. Obviously, such reactions would be most efficient in tissues with low GSH concentrations. In light of the numerous GSH thiol esters likely to be formed from drugs or endogenous carboxylic acids, it is reasonable to speculate that GST-catalyzed hydrolysis of some of these compounds formed in specific tissues or cellular compartments may contribute to the distribution and steady state levels of free acid and GSH conjugate in sites that are remote from their initial sites of ingestion or synthesis.

Details of the catalytic mechanism of thiol ester hydrolysis remain to be determined, but the critical role of Tyr-9 is clear, on the basis of the experiments with the Y9F mutant. In fact, the relative decrease in enzymatic activity when comparing Y9F to the wild type is greater for the thiol esterase activity than for most conjugation reactions catalyzed by GSTA1-1. For the conjugation reactions, the substitution of Tyr-9 with Phe reduces the catalytic activity by 10−50-fold, but some enzymatic activity remains. We estimate that the Y9F mutant is at least 85-fold less efficient than wild type rGSTA1-1 in the hydrolytic reaction, on the basis of the limits of detection of the assay. Thus, Tyr-9 may be considered to be more critical to the GSTA1-1 hydrolysis activity than to its conjugation activity, at least with some substrates. For the hydrolytic reaction described here, several mechanisms are easily envisioned, and include (1) acylation of the tyrosinate-9 anion, followed by hydrolysis of the acyl adduct; (2) general base catalysis by the tyrosinate-9 anion; (3) general acid catalysis by Tyr-9, with proton donation to the thiol leaving group or to the oxyanion formed in the tetrahedral intermediate; and (4) multiple roles for Tyr-9, including both general acid and base catalysis. Each of these mechanisms would be facilitated by the unusually low pK_a of Tyr-9 of the A-class GSTs, ∼8.2. Therefore, it will be of interest to determine the efficiency of other GST isoforms, for which the active site tyrosine has a pK_a of >10, in catalyzing this reaction. Whichever mechanism is operative, several constraints that limit the mechanistic possibilities are provided by the results of the experiments reported here.

The explicit search for an adduct corresponding to acylated Tyr-9 indicates that, if this mechanism is operative, then deacylation does not control the turnover rate. If the majority of GST during the steady state was the acylated Tyr adduct, due to rate-limiting deacylation at 0.1 min^{-1}, then the acylated species would have a half-life of 6.9 min^{-1}. The LC−MS assay developed here included a dead time of 5.1 min between removal of an aliquot at the steady state and ionization. With this dead time, 63% of the protein would remain adducted in MS experiments on the basis of the rate law for irreversible decay of the adduct, $-d[\text{acyl-GST}]/dt = k[\text{acyl-GST}]$. If deacylation of Tyr-9 was catalyzed by the enzyme, then a deacylation rate at least ∼6-fold faster than the turnover rate would be required to eliminate a detectable level of adduct within the experimental dead time, assuming a conservative detection limit of 5% of the total protein existing as an acylated adduct. Thus, the results from these experiments indicate that either acylation of Tyr-9 does not occur or the deacylation is much faster than the overall turnover rate.

Other methods for observing a transiently acylated enzyme will provide increased time resolution. Specifically, rapid quench approaches or stopped flow spectroscopic methods may reveal a kinetic burst corresponding to accumulation of acylated enzyme or released GSH. However, spectroscopic reporters or trapping agents of GSH that are completely stabile and react quantitatively remain to be identified. Therefore, additional effort will be required either to observe such an intermediate or to increase further the lower limit that we can apply to the deacylation rate.

In the absence of a detectable covalent intermediate, and without prior precedent for the active site Tyr of any GST acting as a nucleophilic catalyst, direct hydrolysis of E-SG may be considered the more likely mechanism. Although the isotope tracer experiments described here do not allow for a quantitative analysis of rate constants for partitioning of the initially formed tetrahedral intermediate to GST·E-SG versus GST·EA·GS^-, due to the lack of exchange, a partial qualitative free energy profile can be constructed, using limiting values for the exchange rate and the experimentally determined k_{off}. Figure 6 provides a convenient framework for considering these processes. In Figure 6, a qualitative free energy profile is shown for this mechanism, using the constraints determined experimentally here. In Figure 6, $k_{on} = k_1$ and $k_{off} = k_{-1}$.

For hydrolysis, the partitioning of the tetrahedral intermediate to afford ^{18}O-containing substrate versus hydrolyzed products may be considered as two downhill processes for which the end products, [^{18}O]E-SG or [^{18}O]EA and GSH, are trapped by dilution, and do not re-enter the pool of substrates that contribute to formation of additional ^{18}O-labeled intermediate. Any [^{18}O]E-SG that might be formed

will not effectively compete for binding to the enzyme with the [^{16}O]E-SG that is in vast excess. Similarly, any [^{18}O]EA formed at a low extent of turnover is unlikely to compete for the active site. Therefore, the relative rates of partitioning of the tetrahedral intermediate to the starting thiol ester, k_{-2}, versus hydrolyzed products, k_3, can be estimated from the method of net rate constants (*37*). Under initial velocity conditions, k_{-4} and k_1 approach zero, for any hydrolysis products or ^{18}O-containing thiol ester derived from the tetrahedral intermediate, as a result of the vast excess of [^{16}O]E-SG. The net rate at which the tetrahedral intermediate, TI, partitions to starting thiol ester is described by $[TI]k_{-2}[k_{-1}/(k_{-1} + k_2)]$. Similarly, the net rate of partitioning of TI to hydrolysis products is described by $[TI]k_3[k_4/(k_4 + k_{-3})]$. The limit of detection of ^{18}O in starting thiol ester as determined by the mass spectrometric method used is estimated to be ~1 part in 250. If we account for the statistical factor of 0.5 for the probability that the same oxygen atom introduced from solvent in the TI would be lost upon breakdown (i.e., no enzyme-induced preference), the two expressions must differ by a factor of at least 125.

$$125[TI]k_{-2}[k_{-1}/(k_{-1} + k_2)] = [TI]k_3[k_4/(k_4 + k_{-3})]$$

and

$$125[k_{-1}/(k_{-1} + k_2)]k_{-2} = [k_4/(k_4 + k_{-3})]k_3$$

If we assume that $k_4 \gg k_{-3}$ and on the basis of the experimental values that show that $k_{-1} \gg k_2$, the expression simplifies to $125k_{-2} = k_3$. Apparently, the presumed tetrahedral intermediate formed at the active site nearly completely partitions to hydrolysis products. This result is most striking when compared to the nonenzymatic system, in which the starting thiol ester incorporates ^{18}O during incubation under identical conditions for the same length of time. During this incubation, much less of the starting thiol ester is hydrolyzed than incorporates ^{18}O. In turn, this indicates that the tetrahedral intermediate formed from the specific base-catalyzed (nonenzymatic) reaction preferentially partitions back to the thiol ester, rather than to hydrolysis products. Therefore, the active site dramatically alters the partitioning of the tetrahedral intermediate, which suggests that the enzymatic and nonenzymatic reactions proceed with different mechanisms. An interesting possibility is that the tetrahedral intermediate formed in the enzymatic reaction does, in fact, partition significantly to the starting thiol, but the same atom of solvent-derived oxygen that attacks is specifically expelled such that no ^{18}O is detected in the substrate. Alternatively, tyrosinate-9 may be the nucleophile from which the tetrahedral intermediate is generated, as discussed above. This would preclude ^{18}O incorporation into starting E-SG. In either case, the enzyme does not efficiently control the flux of the tetrahedral intermediate or acylated protein to allow for efficient formation of the GSH ester conjugate. The apparent "one-way flux" of the reaction is not due to rate-limiting release of E-SG, which equilibrates with EA and GSH or EA−GST and GSH at the active site. Rather, the efficient hydrolysis reflects the partitioning of the tetrahedral intermediate or the acylated intermediate to the thermodynamically favored products.

In summary, we report for the first time a GST-dependent hydrolysis of a GSH thiol ester and propose that this catalytic potential could be exploited in the design of GSH-based prodrugs. Furthermore, analogous hydrolytic reactions may contribute to metabolism of endogenous GSH thiol esters. The available data suggest that Tyr-9 of GSTA1-1 acts as a nucleophilic catalyst or a general acid−base catalyst. Whichever mechanism is used, the rate-limiting step is apparently attack of H_2O or Tyr-9 to form the tetrahedral intermediate.

ACKNOWLEDGMENT

We gratefully acknowledge helpful comments provided by each of reviewers.

REFERENCES

1. Hayes, J. D., and Pulford, D. J. (1995) *Crit. Rev. Biochem. Mol. Biol. 30*, 445−600.
2. Armstrong, R. N. (1994) *Adv. Enzymol. Relat. Areas Mol. Biol. 69*, 1−44.
3. Rushmore, T. H., and Pickett, C. B. (1993) *J. Biol. Chem. 268*, 11475−11478.
4. Waxman, D. J. (1990) *Cancer Res. 50*, 6449−6454.
5. Dirr, H., Reinemer, P., and Huber, R. (1994) *Eur. J. Biochem. 220*, 645−661.
6. Armstrong, R. N. (1997) *Chem. Res. Toxicol. 10*, 2−18.
7. Tew, K. D. (1994) *Cancer Res. 54*, 4313−4320.
8. Kolm, R. H., Sroga, G. E., and Mannervik, B. (1992) *Biochem. J. 285*, 537−540.
9. Liu, S., Zhang, P., Ji, X., Johnson, W. W., Gilliland, G. L., and Armstrong, R. N. (1992) *J. Biol. Chem. 267*, 4296−4299.
10. Wang, R. W., Newton, D. J., Huskey, S.-E., McKeaver, B. M., and Lu, A. Y. H. (1992) *J. Biol. Chem. 267*, 19866−19871.
11. Chen, J., and Armstrong, R. N. (1995) *Chem. Res. Toxicol. 8*, 580−585.
12. Meyer, D. J., Crease, D., and Ketterer, B. (1995) *Biochem. J. 306*, 565−569.
13. Zhang, Y., Kolm, R. H., Mannervik, B., and Talalay, P. (1995) *Biochem. Biophys. Res. Commun. 206*, 748−755.
14. Baillie, T. A., and Kassahun, K. (1994) *Adv. Pharmacol. 27*, 163−181.
15. Han, D. H., Pearson, P. G., Baillie, T. A., Dayal, R., Tsang, L. H., and Gescher, A. (1990) *Chem. Res. Toxicol. 3*, 118−124.
16. Ploeman, J. H. T. M., Van Schanke, A., Van Ommen, B., and Van Bladeren, P. J. (1994) *Cancer Res. 54*, 915−919.
17. Phillips, M. F., and Mantle, T. J. (1993) *Biochem. J. 294*, 57−62.
18. Ploeman, J. H. T. M., van Ommen, B., Bagaard, J. J. P., and van Bladeren, P. J. (1993) *Xenobiotica 23*, 913−923.
19. Tew, K. D., Bonber, A. M., and Hoffman, S. J. (1988) *Cancer Res. 48*, 3622−3625.
20. Shore, L. J., Fenselau, C., King, A. R., and Dickinson, R. G. (1995) *Drug Metab. Dispos. 23*, 119−123.
21. Moore, K. H., Tsatsos, P., Staudacher, D. M., and Kielchle, F. L. (1996) *Int. J. Cell Biol. 28*, 183−191.
22. Harris, R. K., and Hamilton, G. A. (1987) *Biochemistry 26*, 1−5.
23. Uotila, L. (1973) *Biochemistry 12*, 3938−3943.
24. Wang, R. W., Newton, D. J., Pickett, C. B., and Lu, A. Y. H. (1991) *Arch. Biochem. Biophys. 286*, 574−578.
25. Atkins, W. M., Wang, R. W., Bird, A. W., Newton, D. J., and Lu, A. Y. H. (1993) *J. Biol. Chem. 268*, 19188−19191.
26. Dietze, E. C., Wang, R. W., Lu, A. Y. H., and Atkins, W. M. (1996) *Biochemistry 35*, 6745−6753.
27. Atkins, W. M., Dietze, E. C., and Ibarra, C. (1997) *Protein Sci. 6*, 873−881.
28. Bjornestedt, A., Sternberg, G., Wilderstern, M., Board, P. G., Sinning, I., Jones, T. A., and Mannervik, B. (1995) *J. Mol. Biol. 247*, 765−773.
29. Jencks, W. P. (1987) *Catalysis in Chemistry and Enzymology*, pp 517−521, Dover Publications, New York.

30. Nieslanik, B. S., and Atkins, W. M. (1998) *J. Am. Chem. Soc. 120*, 6651−6660.
31. Wang, R. W., Bird, A. W., Newton, D. J., Lu, A. Y. H., and Atkins, W. M. (1993) *Protein Sci. 2*, 2085−2094.
32. Lyttle, M. H., Sayton, A., Hozter, M. D., Bauer, K. E., Caldwell, L. G., Hui, H. C., Morgan, A. S., Mergia, A., and Kauvar, L. M. (1994) *J. Med. Chem. 37*, 1501−1507.
33. Jencks, W. P., Cordes, S., and Carriuolo, J. (1960) *J. Biol. Chem. 235*, 3608−3613.
34. Dietze, E. C., Bird, A. W., Ibarra, C., and Atkins, W. M. (1996) *Biochemistry 35*, 11938−11944.
35. Uotila, L., and Koivusalo, M. (1996) in *Enzymology and Molecular Biology of Carbonyl Metabolism*, Vol. 6, Plenum Press, New York.
36. Uotila, L. (1979) *J. Biol. Chem. 254*, 7024−7029.
37. Cleland, W. W. (1975) *Biochemistry 14*, 3220−3224.

BI981284R